Opto-Electronic Advances

Original Article

2019, Vol. 2, No. 3

DOI: 10.29026/oea.2019.180023

All-metallic wide-angle metasurfaces for multifunctional polarization manipulation

Xiaoliang Ma[1,2], Mingbo Pu[1,2], Xiong Li[1,2], Yinghui Guo[1] and Xiangang Luo[1,2]*

Optical camouflage is a magical capability of animals as first noticed in 1794 by Erasmus Darwin in *Zoonomia*, but current biomimetic camouflage strategies cannot be readily applied in complex environments involving multispectral and in particular multi-polarization detection. Here we develop a plasmonic approach toward broadband infrared polarimetric crypsis, where the polarized thermal emission near the pseudo-Brewster angle is the main signal source and no existing polarizing camouflage technique has been discovered in nature. Based on all-metallic subwavelength structures, an electrodynamic resistance-reduction mechanism is proposed to avoid the significant polarization-dependent infrared absorption/radiation. It is also found that the structured metal surface presents giant extrinsic anisotropy regarding the phase shift between orthogonal polarization states, which helps to realize ultrahigh-efficiency and tunable polarization conversion in an unprecedented manner. Finally, we note that the catenary optical theory may provide a useful means to explain and predict these unusual performances.

Keywords: metasurface; polarization; thermal radiation; crypsis; Brewster angle; catenary optics

Ma X L, Pu M B, Li X, Guo Y H, Luo X G. All-metallic wide-angle metasurfaces for multifunctional polarization manipulation. *Opto-Electronic Advances* **2**, 180023 (2019).

Introduction

As one of the most fundamental rules in classical optics, the Fresnel equations, accompanied with Snell's law, determine the reflection and transmission of light incident on an interface of two media with different refractive indices. One important consequence of the Fresnel equations is the Brewster effect, which means the reflectivity for the wave polarized in the plane of incidence (p-polarization) vanishes at a particular incidence angle (Brewster angle). The Brewster effect can be intuitively understood by investigating the elemental dipole radiation[1], which provides many physical insights into this problem. In a more general sense, the modified Brewster effect has been widely utilized to realize extraordinary transmission and broadband angular filters[2,3]. Since the Brewster effect is an interface phenomenon, any modification of the surface conditions would change the light behavior. When a metasurface consisting of periodic or quasi-periodic subwavelength inclusions is inserted at the interface[4–12], the Fresnel equations can be generalized to change the reflection, refraction properties on demand[13].

In the ideal case, the reflectivity of p-polarized wave at the Brewster angle would be zero. However, in general most materials used in optics and electromagnetics are lossy to some extent, thus the minimum reflectivity is not exactly zero. For strongly lossy materials such as metals, the minimal reflectivity is often larger than 10%, thus the corresponding angle is termed pseudo-Brewster angle[14,15]. Note that metal is often treated as a good reflector in most electromagnetic spectrum, thus the reflection minimum seems to be an "abnormal" effect. The energy transmitting into metal would be totally absorbed since there is no way to let them transmit if the metal thickness is larger than the skin depth. This absorption is indeed very strong at the infrared and visible wavelengths, where metal could not be treated as perfect conductors as they were in the microwave range.

The control of the polarization-dependent absorption at pseudo-Brewster angle has great significance in infra-

[1]State Key Laboratory of Optical Technologies on Nano-Fabrication and Micro-Engineering, Institute of Optics and Electronics, Chinese Academy of Sciences, Chengdu, 610209, China; [2]School of Optoelectronics, University of Chinese Academy of Sciences, Beijing 100049, China
*Correspondence: X G Luo, E-mail: lxg@ioe.ac.cn
Received 11 November 2018; accepted 13 January 2019; accepted article preview online 21 February 2019

red applications such as functional devices and infrared polarimetric detection. According to the Kirchhoff's law[16], the thermal emission due to blackbody radiation would also be highly dependent on angle and polarization since the thermal emissivity at infrared region equals to the absorptivity. This also explains why the thermal radiation differs from that described by Lambert's cosine law[17]. As a result, polarimetric imaging could provide a new route for infrared surveillance with the ability to reveal the hidden metallic objects[18].

Here we propose a concept for the design of structured surfaces with inhibited pseudo-Brewster effect. By eliminating the energy loss of surface electromagnetic wave propagating along a structured metallic surface, we show that both the polarimetric thermal emission and laser's reflection loss can be significantly reduced. Consequently, the proposed metasurfaces will serve as an efficient way to modify the polarization states, for either thermal infrared radiation or coherent laser beam.

Results and discussions

To characterize the physical principle of our design, we first consider the Fresnel's reflection at a lossy metal surface under variant angles of incidence. Since the metal is thick enough to absorb the transmitted light, the angle and polarization dependent absorptivity should be:

$$A_{\mathrm{s}} = 1 - \left(\frac{\sqrt{\varepsilon_{\mathrm{m}} - \sin^2\theta} - \cos\theta}{\sqrt{\varepsilon_{\mathrm{m}} - \sin^2\theta} + \cos\theta} \right)^2 , \qquad (1)$$

and

$$A_{\mathrm{p}} = 1 - \left(\frac{\varepsilon_{\mathrm{m}}\cos\theta - \sqrt{\varepsilon_{\mathrm{m}} - \sin^2\theta}}{\varepsilon_{\mathrm{m}}\cos\theta + \sqrt{\varepsilon_{\mathrm{m}} - \sin^2\theta}} \right)^2 , \qquad (2)$$

where A_{s} and A_{p} are the absorptivity for s and p polarized waves, ε_{m} and θ are the permittivity of the metal as well as the incidence angle. When $|\varepsilon_{\mathrm{m}}|$ is much larger than unity and possesses negligible loss, A_{s} is almost zero for all angle of incidence. For the p-polarized light, it is well-known that there is a special angle where the reflectance is at minimum. Different from the Brewster effect for transparent dielectrics, the complex permittivity of metal makes the reflectivity minimum not to be exactly zero[14]. Obviously, the pseudo-Brewster's effect is responsible for the large energy loss for p-polarized light at oblique incidence, which would be harmful to the optical performance of omnidirectional reflectors and other reflective optical devices. More importantly, this polarization-dependent absorption could also lead to highly polarized infrared radiation at thermal equilibrium, forming a huge obstacle for polarization camouflage against infrared detection[19].

In a phenomenological view, the increased absorption at the pseudo-Brewster angle is associated with the large vertical electric fields E_z above the metal surface (Fig. 1(a)), which makes the horizontal wave impedance matched to that of metal[13]. To eliminate these vertical fields, periodic metallic posts have been introduced on the surface. As can be seen in Fig. 1(b), the posts have intrinsic plasmonic modes propagating vertically in the posts array[20]. Since the electric fields are perpendicular to the vertical axis, E_z is forced to vanish at the surface, which helps to reduce the absorption as well as the thermal emission. Interestingly, this coupled plasmonic modes have a feature of catenary optical fields[21–24], which provides a universal and useful method for the fast calculating of the optical performance. As shown in our recent work[25], the semi-analytic description of our current all-metallic structures is possible.

To prove the above hypothesis, a full-wave finite-element method (FEM) is adopted to solve the Maxwell's Equations in the structured surface rigorously[26]. The results have also been compared with theoretical model that approximate the structured surface to be an equivalent boundary condition. As depicted in Figs. 2(a) and 2(b), we first considered the angle-resolved reflectivity at λ= 10.6 μm for both the s- and p- polarizations at a smooth and a structured gold surfaces, respectively. The pseudo-Brewster angle for the smooth gold surface is about 86°, coinciding well with the large-index approximation. The p-polarized reflectivity at this angle is only about 50%, implying a strong ohmic loss in this case. For

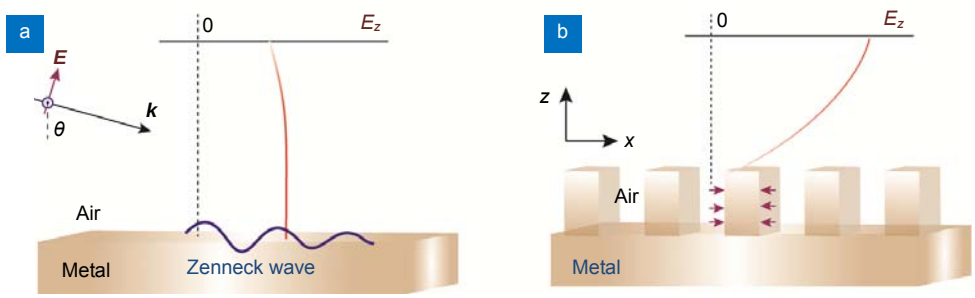

Fig. 1 | (**a**) Electromagnetic reflection on a flat surface at the pseudo-Brewster angle. Note that the reflection minimum is related to the Zenneck surface wave that propagates along the interface between air and a lossy smooth metal. (**b**) Electric field distribution at the pseudo-Brewster angle for a posts array.

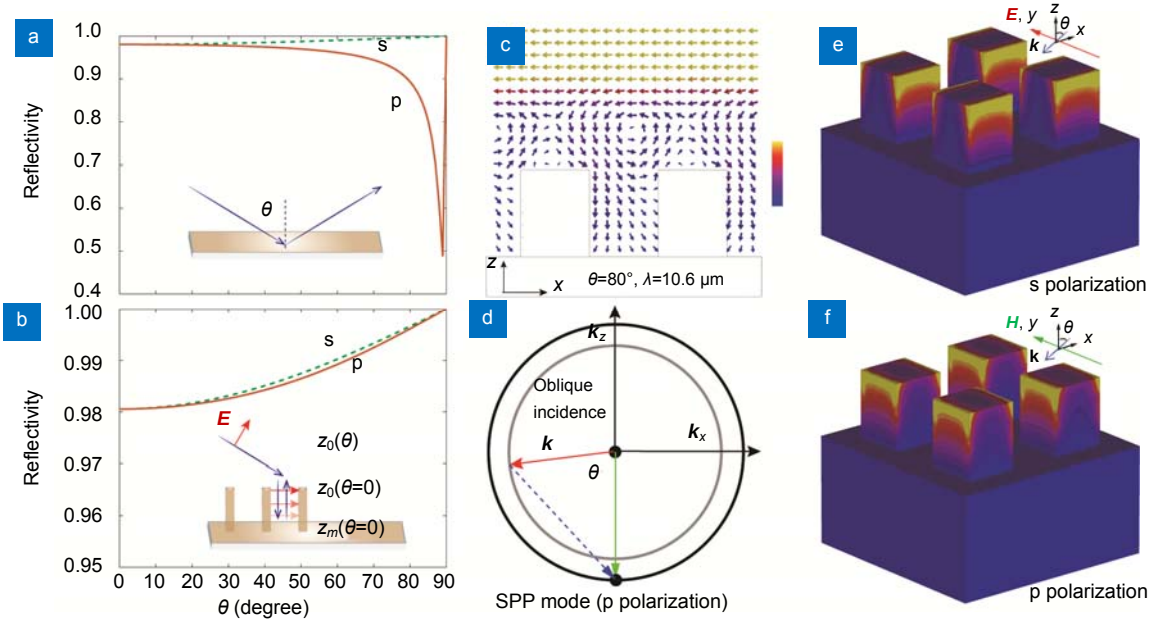

Fig. 2 | Theoretical analysis of the metallic grating. (**a**) Reflectance of s- and p-polarized light for a smooth gold plate. (**b**) Reflectance of s- and p-polarized light for a gold plate decorated with subwavelength posts array. (**c**) Energy flow in the *xz*-plane when p-polarized light is incident with a angle of 80°. (**d**) Schematic of the wavevector mismatching at the air-posts interface. (**e**) and (**f**) Amplitudes of the electric fields for s- and p-polarization at θ=80°.

a periodic rectangular posts array with a period of 3 μm, a height of 1.9 μm and a width of 1.25 μm, the absorption peaks become nearly completely eliminated, while the reflectivity for the two polarizations are the same for almost all angles of incidence (Fig. 2(b)).

Figure 2(c) depicts the energy flow of the p-polarized light with an incident angle of 80°, which could provide a visual understanding of the new boundary layer. Two signatures should be noted in the power flow: First, there is clear vortex flows just above the posts array; second, only very small part of energy is directed into the gaps between the posts. The vortex is similar to the fluid dynamics when the surface roughness is larger than the molecules of fluid[27], which forms a virtual boundary to reflect light away. The small energy penetration can be rigorously interpreted by considering the horizontal wave vector of the electromagnetic wave. As illustrated in Fig. 2(d), the wavevector in the posts array is perpendicular to the surface for p-polarization and presents a huge mismatch with that of the incidence wave, leading to a dramatic reflection at the first interface between air and the posts array. More precisely, the optical performance of the posts array can be analyzed using a simple impedance model and transfer matrix method. It is interesting to observe that the width and period of the posts have only small influence on the impedance. As a result, the performance of the device is rather robust against fabrication error (see Supplementary information for detail).

One fascinating property of the reflection spectra shown in Fig. 2(b) is that the curves for the two polarizations virtually overlap with each other. This can be understood from the super-symmetry of the plasmonic modes, which is very useful in many flat optical metasurfaces[28,29]. Owing to the two-dimensional periodicity, the surface is intrinsically independent of polarization at normal incidence. At oblique incidence, the ohmic loss is also identical for orthogonal polarizations owing to the symmetry of the plasmonic modes, which is depicted in Fig. 2(e) and 2(f), for θ=80°. As can be further demonstrated, the de-polarization effect is also a broadband phenomenon (Fig. S1), which makes it an ideal candidate for broadband infrared crypsis.

In our experiments, the posts array was fabricated by triple resist technology followed by laser direct writing and electron beam deposition (Fig. S2). The SEM image of a sample coated with gold is shown in Fig. 3(a). The reflectance for different incident angles and polarizations measured by Fourier transform infrared spectroscopy (FTIR) are shown in Figs. 3(b) and 3(c), showing good agreement with our theoretical results. The slightly increased absorption is attributed to the finite thickness and surface roughness of the metallic coating layer. Owing to the angle limitation of our FTIR, instead of the reflectance at the pseudo-Brewster angle, only the cases at 70° and 80° were measured.

The metallic posts array can be used to suppress the p-polarized thermal radiation near the pseudo-Brewster angle. We note that this directive and polarized thermal radiation of flat metal surface have been observed by Arago in almost two hundred years ago[30], in stark contrast to the Lambert's radiation law as well as the common sense about the spatial coherence of thermal radiation[31]. It was recently realized that the Lambert's cosine law is only valid for perfect black body, thus nearly all

manmade objects would have directive and polarized emission to some extent[16]. For the thermal radiation of a metal surface, the physical process can be viewed in a different picture: the total thermal emission can be considered as the black-body radiation that transmitted from metal to air[32]. Different from the coherent thermal emission assisted by surface-phonon polaritons[31], the directive and polarized thermal emission of flat metal surface can be ascribed to the excitation of Zenneck surface wave at the pseudo-Brewster angle[33,34].

To demonstrate the suppressed unusual thermal radiation, the infrared images of a posts array (Fig. 3(d)) and a reference plate coated with 200 nm thick chromium are captured by an infrared polarimetric imaging system (Fig. S3). The chromium is chosen because it has much larger ohmic loss and more obvious thermal emission than gold. The temperature is set to be 50 degrees centigrade, corresponding to black radiation centered at about λ=9 μm. The measured thermal emission angle with respect to the normal axis is near 70°. As shown in Figs. 3(e) and 3(f), the emission intensity for the structured sample are almost identical for the two polarizations (see Fig. S4 for the measured broadband spectra). Unlike the structured sample, the flat surface has much stronger intensity for p-polarization, which is a significant signal for infrared target recognition.

Although there are almost no difference between the reflectance and absorbance between the p- and s-polarizations for all incidence angles, some relative phase shift would occur between the two polarized components. This can be well characterized by our impedance model. As depicted in Fig. 4, the theoretical results agree well with the FEM calculations at λ=10.6 μm, which indicate an increasing phase difference along with the rise

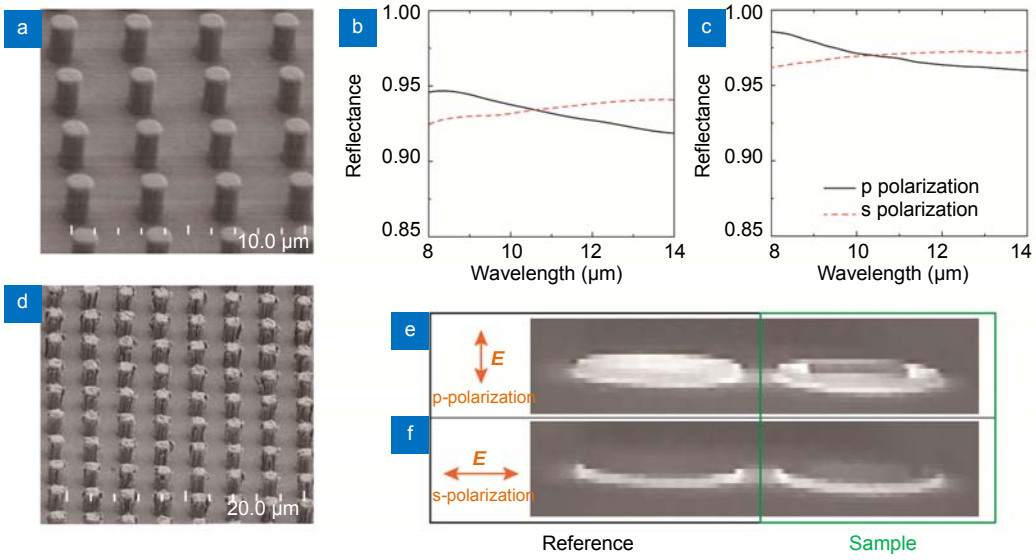

Fig. 3 | Broadband reflectance and polarimetric imaging. (**a**) Perspective view of the gold-sample. (**b**) and (**c**) FTIR spectra of the gold sample for incidence angles of 70° to 80°. The p- and s-polarizations are indicated in each panel. (**d**) Perspective view of the chromium sample. (**e**) and (**f**) Polarized infrared images of the chromium-sample and a reference sample for p- and s- polarizations. The strong emission at the circumference of the sample is from the silicon dioxide substrate (the diameter of the substrate is 2.5 cm and the structured is fabricated in a square region with a width of 1.5 cm).

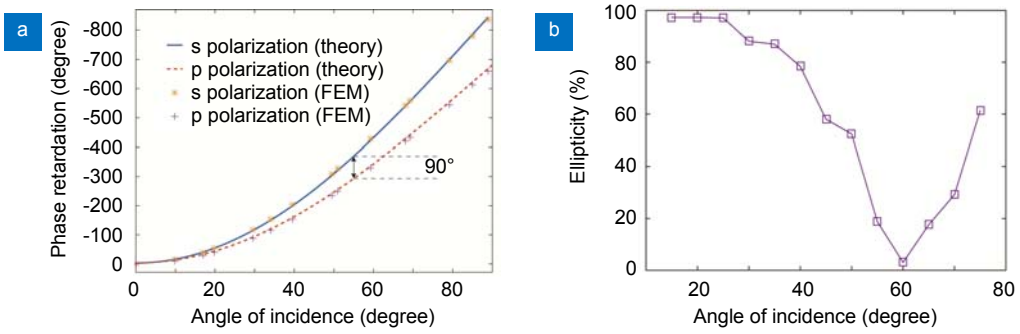

Fig. 4 | Metallic posts array acting as a reflective waveplate. (**a**) Reflective phase retardation at different incidence angles for s- and p-polarizations at λ=10.6 μm. The distance between the reference plane and the top of the posts array is 10 μm. The theory is based on the effective impedance and transfer matrix method. (**b**) Measured ellipticity of the reflected laser beam generated by a CO_2 laser (λ=10.6 μm).

of incidence angle. At almost θ=56°, the phase difference is about 90°, meaning that the corrugated surface can act as a highly efficient reflective quarter waveplate. The polarization ellipticity, defined as $(I_{max}-I_{min})/(I_{max}+I_{min})$ (I_{max} and I_{min} are the maximum and minimum intensities when rotating the polarizer), is measured at λ=10.6 μm for different incidence angle (Fig. S5). As shown in Fig. 4(b), the ellipticity reaches the minimum of about only 1% at θ=60°. It is interesting to note that the sample is isotropic in the *xy*- plane, from which one may expect that the posts array should be highly anisotropic in the *xz*- and *yz*-plane[35]. Since the anisotropy takes place only for off-axis illumination, this polarization conversion effect is termed extrinsic anisotropy, similar to the definition of extrinsic chirality[36]. We note that the polarizing mirror can also operate in a broadband spectrum. By varying the angle of incidence, the operating wavelength can be tuned from 7 μm to almost 24 μm (Fig. S6).

Conclusions

In summary, the most remarkable feature of the results shown in this paper is that the pseudo-Brewster effect can be nearly completely eliminated, leading to significantly reduced and non-polarized thermal emission and providing an important means to achieve polarimetric crypsis. This simple structure is also easy to fabricate in large volume for practical applications. Besides the camouflage applications, we showed that the same surface-relief structure can be used as a highly-efficient reflective mirror, which could generate circular polarization in a broadband spectrum. Different from the anisotropic metamirror[37,38], this phenomenon might be described by the extrinsic anisotropy and regarded as a generalization of the Brewster' law[1].

References

1. Paniagua-Domínguez R, Yu Y F, Miroshnichenko A E, Krivitsky L A, Fu Y H *et al*. Generalized Brewster effect in dielectric metasurfaces. *Nat Commun* **7**, 10362 (2016).
2. Alù A, D'Aguanno G, Mattiucci N, Bloemer M J. Plasmonic Brewster angle: broadband extraordinary transmission through optical gratings. *Phys Rev Lett* **106**, 123902 (2011).
3. Shen Y C, Ye D X, Celanovic I, Johnson S G, Joannopoulos J D *et al*. Optical broadband angular selectivity. *Science* **343**, 1499–1501 (2014).
4. Yu N F, Genevet P, Kats M A, Aieta F, Tetienne J P *et al*. Light propagation with phase discontinuities: generalized laws of reflection and refraction. *Science* **334**, 333–337 (2011).
5. Pu M B, Li X, Ma X L, Wang Y Q, Zhao Z Y *et al*. Catenary optics for achromatic generation of perfect optical angular momentum. *Sci Adv* **1**, e1500396 (2015).
6. Tang D L, Wang C T, Zhao Z Y, Wang Y Q, Pu M B *et al*. Ultrabroadband superoscillatory lens composed by plasmonic metasurfaces for subdiffraction light focusing. *Laser Photonics Rev* **9**, 713–719 (2015).
7. Minovich A E, Miroshnichenko A E, Bykov A Y, Murzina T V, Neshev D N *et al*. Functional and nonlinear optical metasurfaces. *Laser Photonics Rev* **9**, 195–213 (2015).
8. Qin F, Ding L, Zhang L, Monticone F, Chum C C *et al*. Hybrid bilayer plasmonic metasurface efficiently manipulates visible light. *Sci Adv* **2**, e1501168 (2016).
9. Ma Z J, Hanham S M, Albella P, Ng B, Lu H T *et al*. Terahertz all-dielectric magnetic mirror metasurfaces. *ACS Photonics* **3**, 1010–1018 (2016).
10. Chu C H, Tseng M L, Chen J, Wu P C, Chen Y H *et al*. Active dielectric metasurface based on phase-change medium. *Laser Photonics Rev* **10**, 986–994 (2016).
11. Bao Y J, Zu S, Liu W, Zhou L, Zhu X *et al*. Revealing the spin optics in conic-shaped metasurfaces. *Phys Rev B* **95**, 081406 (2017).
12. Jiang Q, Bao Y J, Lin F, Zhu X, Zhang S *et al*. Spin-controlled integrated near- and far-field optical launcher. *Adv Funct Mater* **28**, 1705503 (2018).
13. Luo X G. Principles of electromagnetic waves in metasurfaces. *Sci China Phys Mech Astron* **58**, 594201 (2015).
14. Ohman G. The pseudo-brewster angle. *IEEE Trans Antennas Propag* **25**, 903–904 (1977).
15. Azzam R M A. Complex reflection coefficients of p- and s-polarized light at the pseudo-Brewster angle of a dielectric–conductor interface. *J Opt Soc Am A* **30**, 1975–1979 (2013).
16. Liu X L, Tyler T, Starr T, Starr A F, Jokerst N M *et al*. Taming the blackbody with infrared metamaterials as selective thermal emitters. *Phys Rev Lett* **107**, 045901 (2011).
17. Worthing A G. Deviation from lambert's law and polarization of light emitted by incandescent tungsten, tantalum and molybdenum and changes in the optical constants of tungsten with temperature. *J Opt Soc Am* **13**, 635–649 (1926).
18. Pezzaniti J L, Chenault D, Gurton K, Felton M. Detection of obscured targets with IR polarimetric imaging. *Proc SPIE*, **9072**, 90721D (2014).
19. Tyo J S, Goldstein D L, Chenault D B, Shaw J A. Review of passive imaging polarimetry for remote sensing applications. *Appl Opt* **45**, 5453–5469 (2006).
20. Wang K L, Mittleman D M. Metal wires for terahertz wave guiding. *Nature* **432**, 376–379 (2004).
21. Pu M B, Guo Y H, Li X, Ma X L, Luo X G. Revisitation of extraordinary young's interference: from catenary optical fields to spin–orbit interaction in metasurfaces. *ACS Photonics* **5**, 3198–3204 (2018).
22. Luo X G. Subwavelength artificial structures: opening a new era for engineering optics. *Adv Mater* **25**, 1804680 (2019).
23. Luo X G, Tsai D, Gu M, Hong M H. Subwavelength interference of light on structured surfaces. *Adv Opt Photonics* **10**, 757–842 (2018).
24. Rahmani M, Leo G, Brener I, Zayats A V, Maier S A *et al*. Nonlinear frequency conversion in optical nanoantennas and metasurfaces: materials evolution and fabrication. *Opto-Electron Adv* **1**, 180021 (2018).
25. Xie X, Pu M B, Huang Y J, Ma X L, Li X *et al*. Heat Resisting Metallic Meta‐Skin for Simultaneous Microwave Broadband Scattering and Infrared Invisibility Based on Catenary Optical Field. *Adv Mater Technol*, 1800612 (2018). https://doi.org/10.1002/admt.201800612
26. CST Microwave Studios. CST-Computer Simulation Technology AG, 2013.
27. Granick S, Zhu Y X, Lee H. Slippery questions about complex fluids flowing past solids. *Nat Mater* **2**, 221–227 (2003).

28. Pu M B, Li X, Guo Y H, Ma X L, Luo X G. Nanoapertures with ordered rotations: symmetry transformation and wide-angle flat lensing. *Opt Express* **25**, 31471–31477 (2017).
29. Guo Y H, Ma X L, Pu M B, Li X, Zhao Z Y *et al*. High‐efficiency and wide‐angle beam steering based on catenary optical fields in ultrathin metalens. *Adv Opt Mater* **6**, 1800592 (2018).
30. Sandus O. A review of emission polarization. *Appl Opt* **4**, 1634–1642 (1965).
31. Greffet J J, Carminati R, Joulain K, Mulet J P, Mainguy S. Coherent emission of light by thermal sources. *Nature* **416**, 61–64 (2002).
32. Joulain K, Mulet J P, Marquier F, Carminati R, Greffet J J. Surface electromagnetic waves thermally excited: radiative heat transfer, coherence properties and Casimir forces revisited in the near field. *Surf Sci Rep* **57**, 59–112 (2005).
33. Polo J A Jr, Lakhtakia A. Surface electromagnetic waves: a review. *Laser Photonics Rev* **5**, 234–246 (2011).
34. Barlow H M, Cullen A L. Surface waves. *Proc IEE - Part III Radio Commun Eng* **100**, 329–341 (1953).
35. Shin J, Shen J T, Catrysse P B, Fan S H. Cut-through metal slit array as an anisotropic metamaterial film. *IEEE J Sel Top Quantum Electron* **12**, 1116–1122 (2006).
36. Plum E, Fedotov V A, Zheludev N I. Optical activity in extrinsically chiral metamaterial. *Appl Phys Lett* **93**, 191911 (2008).
37. Pu M B, Chen P, Wang Y Q, Zhao Z Y, Huang C *et al*. Anisotropic meta-mirror for achromatic electromagnetic polarization manipulation. *Appl Phys Lett* **102**, 131906 (2013).
38. Grady N K, Heyes J E, Chowdhury D R, Zeng Y, Reiten M T *et al*. Terahertz metamaterials for linear polarization conversion and anomalous refraction. *Science* **340**, 1304–1307 (2013).

Acknowledgements

We acknowledge the financial support by National Natural Science Foundation of China under contact Nos. 61622508, 61622509, and 61675208.

Competing interests

The authors declare no competing financial interests.

Supplementary information

Supplementary information for this paper is available at https://doi.org/10.29026/oea.2019.180023